



Development of A Filament Extruder Using Flow Theory with The Newtonian Fluid Assumption

Nien Thi Nguyen¹, Chinh Truong Van¹, Trieu Khoa Nguyen^{1*}

¹Faculty of Mechanical Engineering,
Industrial University of Ho Chi Minh City, Ho Chi Minh City, 70000, VIETNAM

*Corresponding Author

DOI: <https://doi.org/10.30880/ijie.2023.15.07.011>

Received 23 November 2023; Accepted 17 October 2023; Available online 5 December 2023

Abstract: This article presents an investigation into the flow characteristics of polymer melt in a single-screw extruder and outlines the design of a filament extruder to validate the aforementioned theory. The flow characteristics of the polymer melt in a single-screw extruder resemble those of a viscous liquid confined between two infinitely parallel sheets, with one sheet in motion and the other stationary. An integrated flow equation is derived for the scenario where the viscosity of the liquid remains constant during isothermal extrusion. These theories governing flow behavior are subsequently verified through the design and construction of a filament extruder intended for use in 3D printers.

Keywords: Filament extruder, Newtonian fluid, polymer melt, flow behavior, 3D printing

1. Introduction

Manufacturing methodologies employing screws, such as extrusion and injection molding, are experiencing growing indispensability across various industrial sectors, including plastic wares, food processing, and the development of feeders for ancillary machinery. Furthermore, the utilization of such techniques is anticipated to witness a substantial increase in forthcoming applications [1]. Among the diverse array of screw-based machines employed in industry, single-screw extruders stand out as the predominant and extensively researched category [1]. The theoretical framework governing fluid dynamics within a single-screw extruder can be classified into two branches.

Firstly, molten plastic was considered a Newtonian fluid. As early as the 50s, J. F. Carley and R. A. Strub [2] had in-depth studies of molten plastic flow in a single screw extruder using the Newtonian fluid assumption. Meanwhile, also assuming that molten plastic was an incompressible fluid, R.M. Griffith [3] uses power equations and the integrated Runge-Kutta method to approximate solutions. As a result, these equations were too complex to be applied in practice. It was worth noting that many authors developed their own mathematical models, without using the continuity equation of the extruder. An elaborate study by D. J. Weeks and W. J. Allen [4] consisted of two parts, the development of a Newton flow theory and the verification using a non-Newtonian fluid extrusion experiment of polythene. The accuracy of the model was within 25%, however, the model was also too complicated to apply in practice. Similarly, Y. Li and F. Hsiel [5] developed a new mathematical model to calculate the flow of isothermal and incompressible Newton fluids inside a single-screw extruder. Next, Campbell G.A. et al. [6] studied the flow of molten plastic in an extruder with a screw diameter of 49.66 mm. Although their equation was simple, the applicability was not high because the screw diameter itself was an input parameter, and it was necessary to estimate/measure the drag force and the reaction impact on the screw. As a continuation of their studies, J. F. Carley et al. [7] found a simplifying theory for the flow of Newtonian fluids in single-screw extruders using partial differential equations. Recently, Christian Marschik et al. also used Newtonian fluid theory to perform their research. Their publication was divided into 2 parts, part A [8] was the in-depth research on flow theory to reduce the complexity of the mathematical models, and part B [9] presented new developments

of the drag flow in a single screw extruder. However, their important input parameter was the diameter of the screw, 35 mm, the outputs were equations describing the fluid flow, which were difficult to be applied by students or engineers.

Secondly, molten plastic was considered a non-Newtonian fluid. In fact, most molten plastics were non-Newtonian fluids and, therefore, assuming they had Newtonian properties would lead to significant errors [10]. Consequently, the fluid flow theories in screw extruders were extended to deal with non-Newtonian fluids. Since the early 60s, P. H. Squires [11] assumed the fluid flow in screw extruders was non-Newtonian and non-isothermal. Since the extruded fluid was non-Newtonian, the viscosity varied at different positions in the extruder due to the variation of shear stress. And the author proposed to calculate the correction factor F_{DC} for the screw blade shape. Therefore, although using the extruder continuity equation, the results of this author were too complicated to be applied in design. Also used the theory of non-Newtonian fluids and non-isothermal, but R. T. Fenner and J. G. Williams [12] used power functions to express the relationship between shear stress τ and shear rate $\dot{\gamma}$. Therefore, the partial differential equations of this study were difficult to take into account in real design. In another work, R. Brzoskowski et al. [13] presented a simple mathematical model to describe non-Newtonian isothermal flow for the metering zone of the extruder. The authors used a 1.5" diameter screw for the investigation. And from this mathematical model, it was not possible to perform a reverse computation for the required screw diameter. Therefore, it was not highly applicable to design works. Many other authors also used non-Newtonian fluid theory for their studies. Acur, E.E., and Vlachopoulos, J. [14] utilized non-Newtonian fluid theory to simulate the screw extrusion process, thereby forming partial differential equations describing the mass, moment, and energy of molten plastic. A screw with a diameter of 38 mm was used as the key input. However, calculating screw diameter from the above partial differential equations was very complicated. And C. Rauwendaal [10] utilized a finite element software solution to analyze the flow and heat transfer of molten plastic in the extruder. These analyzes were also difficult to replicate on-site. Also simulating, Wang, Y., and Tsay, C.C. from Taiwan used the Newton-Raphson iteration method to solve power equations to study the mixing modes in the extruder, Maddock, Dulmage, and the blister ring [15]. An extrusion screw with a diameter of 35 mm was utilized in this study. Because the purpose of this study was to model the flow of molten resin to study the mixing modes, these results could not be directly applied to design work. Also using a finite element software solution, Naksoo Kim et al. [16] utilized the Carreau-Yasuda model to describe the viscosity of the molten resin and the quadratic integrated Runge-Kutta numerical method to solve it. Similarly, in [17], Marschik, Christian et al. simulated the non-Newtonian flow of shear-thinning polymer melt. And the combination of partial differential functions and ternary polynomial functions in this study limited its applicability in the selection of screw diameters. Next, Wilczyński, Krzysztof et al. from Poland [18] simulated the wood-plastic composite extrusion process. The model they came up with could predict extrusion capacity, pressure, temperature, melting process as well as energy consumption. They also did a validation experiment using a screw with a diameter of 45 mm. However, the diameter of the screw could not be calculated from parameters such as extrusion capacity, pressure, and temperature, so this model could be difficult to be used for design and fabrication. After that, these authors continued to improve their mathematical model in the next publication [19]. However, due to their research objectives and the mathematical model itself, their contribution to both practical and academic fields was not high.

It should be noted that many studies used both Newtonian and non-Newtonian flow theory. The study of the authors Weeks and Allen [4] consists of two parts, developed Newton flow theory and re-tested by non-Newtonian fluid extrusion experiment using polythene. In review articles on extrusion, for example, the authors in [20] synthesized and analyzed 77 studies on extrusion, both using Newtonian and non-Newtonian fluid theory. Through this overview, most of the studies using non-Newtonian fluid theory had quite complicated mathematical models. Despite being highly academic, they were difficult to use for teaching or for the field engineer to choose the screw diameter.

As mentioned above, the screw extrusion technique is widely used in both industrial and civil applications. In particular, the screw extrusion technique has been utilized a lot in a very noticeable technology today, 3D printing technology, to produce plastic filaments for printers. 3D printing is a technology that produces objects by placing materials in layers. Each layer is a thin cross-section of the object, computer-generated [21, 22]. The outstanding advantages of 3D printing technology are to help shorten the development time; quickly produce products in small quantities; help speed up the process of bringing products to market; reduce costs with better quality and better designs; optimize product inspection and modification (the ability to create real products directly from the drawing). With this technology, it is possible to fabricate objects with exceptionally complex, sophisticated, and precise structures that cannot be done by traditional machining methods. In addition, 3D printing technology has almost no waste of construction materials or scaffolding; helps protect workers' health; and reduces transportation costs, and CO2 emissions. 3D printing technology has gained promising developments - the technology for the future that turns all human ideas into reality [23, 24]. It can be said that 3D printing technology is the key technology of Industrial Revolution 4.0.

Therefore, there have been many studies on the design and manufacture of plastic filament extruders for 3D printers. In a book chapter specializing in addition manufacturing [25], Kamaljit Singh Boparai and Rupinder Singh presented the design and fabrication of a filament extrusion equipment for an FDM (fused deposition modeling) 3D printer. The device had a screw diameter of 25 mm. However, the calculation process for this diameter was not shown. While Harimalairajan K. et al. from India [26] built a plastic filament extruder for a 3D printer with a rather large 65 mm screw and the screw rotation speed of the screw was 20 revolutions per minute. However, the authors also did not show the calculating step to design the screw. With a more expensive cost, approximately \$ 700, Woern et al. [27] have developed a recycled

plastic extrusion system, which includes a filament winding system after being extruded. However, also as above, the reason why the screw has a diameter of 5/8" wasn't shown. Also, for the recycling of plastic, in [28], Mazher Iqbal Mohammed et al. developed a device to recycle ABS plastic from electronics. Solar energy was used for eco-friendly printing. In [28], these authors also did not show the diameter calculation of screw design. Also aiming to be environmentally friendly, Sean Whyman et al. [29] have developed a 3D printer using granular bioplastics. And in the design of the screws, they also did not present the calculation to achieve this diameter. In the extrusion processing guide and handbook, screw design chapter [30], screw diameter was selected based on a graph with extrusion capacity pounds/hour as the input parameter. The vertical axis of the graph had a log scale, so the table lookup was not completely accurate. And the authors did not show the theoretical basis for this graph.

As mentioned, the investigations of molten plastic flow in the extrusion equipment were highly academic, and therefore, were quite complex. In order to apply these theories to the screw diameter calculation for the extruder design, the continuity equation of the extrusion process was used with the Newton fluid assumption. The integrated flow equation was then found for a case where the viscosity of the liquid remained constant in the isothermal extrusion. Next, from this equation, the screw diameter was calculated and selected based on a number of design requirements. These equations were then verified via a screw design for a plastic filament extruder for an FDM 3D printer. The results showed that the established screw diameter calculation equation was suitable for students or engineers to estimate and select the screw diameter and then calculated other parameters of the extruder.

2. Flow Theory for Polymer Melt and Its Application for Screw Design

2.1 Newtonian Fluid

It was early discovered that within the fluid between two parallel flat plates, one fixed plate, and one moving plate, some liquid was pulled by the moving plate. Newton proposed the concept of shear stress, τ , between two adjacent fluid layers that was proportional to the gradient or shear rate, ds/dy [2].

$$\tau = \mu \frac{ds}{dy} \quad (1)$$

A fluid that satisfies Eq. (1) is called Newtonian fluid. And the rate constant, μ , denotes the viscosity coefficient or shortly the viscosity of the fluid. The viscosity of a fluid is inversely proportional to the temperature. For many fluids, the value μ is not a constant but relies on the shear stress or shear rate. In some fluids, μ is affected by the time that the fluid is stressed.

2.2 Fluid Flow in a Single Screw Extruder

The flow mechanism of the polymer melt in the screw channel can be easier figured out when one assumes the channel is unrolled and spread on a plane. Fig. 1 shows a diagram for this assumption. Fig. 1(a) shows the polymer in the channel is unrolled and spread straight. And Fig. 1(b) presents the cross-section of the channel perpendicular to the unrolled polymer straight line. The upper plate represents the barrel surface, which is traveled in the direction that makes an angle φ to the cross-section. Hence, this relative movement will be similar to what happens in the extruder when the barrel is stationary, while the screw is rotating. When the fluid wets both surfaces, the movement of the barrel will drag the fluid along with it. Whereas the stationary surface creates an equal and opposite resistance to the drag. The velocity of the fluid, relative to the screw, is maximized at the body surface and zero on the screw surface. The direction of the flow is also a relevant factor because the channel is tilted at an angle φ relative to the direction of movement. Hence, when calculating the flow rate inside the canal, the velocity is divided into two components: one axial impact down the channel, the other in a perpendicular direction. The component acting down the channel is called the drag velocity, while the perpendicular component is the transverse velocity. There is usually an extrusion head or die that restricts the flow at the end of the channel. This creates a differential pressure (pressure gradient), generating a flow in the opposite direction of the drag flow. It can be called pressure flow. In addition, there is one more flow that needs attention. Usually, the screw is not assembled perfectly into the barrel. Hence, there is a small gap between the top of the flight of the screw and the inner surface of the barrel. The viscous polymer melt will tend to leak through these gaps because of the pressure difference along the screw. It is called leak flow.

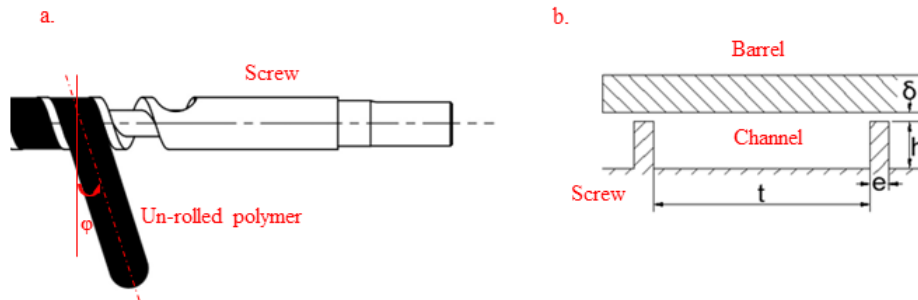


Fig. 1 - Screw channel diagrams (a) un-rolled polymer; (b) respective channel

The productivity of the extruder (Q) is the algebraic sum of the drag flow (Q_D), the pressure flow (Q_P), and the leak flow (Q_L). Eq. (2) denotes the flow equation for the extrusion, which is actually a mass conservation equation based on the uncompressed fluid assumption [7].

$$Q = Q_D - Q_P - Q_L \tag{2}$$

The leak flow can be neglected because its value is usually very small compared to other flows [4]. The velocity of the fluid at any point in the screw channel changes with its position and depth. Equation 3 describes this two-dimensional velocity distribution:

$$\frac{\partial^2 v}{\partial^2 x} + \frac{\partial^2 v}{\partial^2 y} = \frac{1}{\mu} \left(\frac{dP}{dz} \right) \tag{3}$$

This is the differential equation established by Navier in 1822, the general flow equation for Newton fluids [2]. Where z is the distance measured along the helix of the channel and v is the velocity of any point in the channel. Assuming that the influence of the channel wall on the velocity distribution is trivial, these flow equations can be greatly simplified. In other words, the problem is simplified by assuming that a special case of infinite parallel sheets is utilized. Hence, the velocity distribution becomes one-dimension. For screws with shallow channels, the error due to this approximation is considered quite small. As the ratio of width and depth is greater than or equal to 10, the error is shown less than 10% [7]. In plastic extrusion technology, most used screws fall into this category and therefore simplified flow equations are very useful for design (calculation of screw diameter) and other applications. From Eq. (3), the differential equation introducing the one-dimensional velocity distribution can be achieved by giving the second derivative of velocity corresponding to x equal to zero. Eq. (3) becomes [2]:

$$\frac{\partial^2 v}{\partial^2 y} = \frac{1}{\mu} \left(\frac{dP}{dz} \right) \tag{4}$$

By integrating Eq. (4) twice, Eq. (5) - velocity at any point on the channel in the extruder is achieved as:

$$v = \frac{vy}{h} + \frac{(y^2-hy)}{2\mu} \left(\frac{dP}{dz} \right) \tag{5}$$

h is the height of the flight of the screw. On the surface of the barrel, when $y = h$, the velocity of the liquid is equal to V (relative to the screw). While at the surface of the screw, where $y = 0$, the liquid velocity is equal to zero. In the Eq. (5), the first term on the right side is the velocity of the drag flow while the second term denotes the velocity of the pressure flow. Fig. 2 shows the velocity plots of these two flows. The velocity of the drag flow changes linearly with the depth of the channel. Whereas the distribution of the pressure flow is parabolic. Hence the sum of these two fluid-flows results in the actual velocity at each point. The flow volume equation is generated from the velocity equation using the integration of the area-velocity product from the top to the bottom of a screw channel. Eqs. (6), (7), and (8) represent this process:

$$Q = \int_0^h v w dy \tag{6}$$

$$Q = w \int_0^h \left[\frac{vy}{h} + \frac{(y^2-hy)}{2\mu} \left(\frac{dP}{dz} \right) \right] dy \tag{7}$$

$$Q = \frac{vwh}{2} - \frac{wh^3}{12\mu} \left(\frac{dP}{dz} \right) \quad (8)$$

Where w denotes the width of the channel flight measured in a line perpendicular to the pitch axis of the screw. The helix angle of the screw flight is denoted as ϕ . The first term on the right side of Eq. (8) denotes the drag flow rate and then the pressure flow rate. Eq. (8) can be taken to a simpler form when the shape of the screw thread is taken into account. In this case, screws with one or more screw flights can also be studied. A schematic diagram of a two-flight screw which is the simplest multi-flight screw, is shown in Fig. 3. When the threads from one section of the considered screw, that is the same length as the lead, are unrolled from the root of the screw and laid flat, the illustration will be as in Fig. 3.

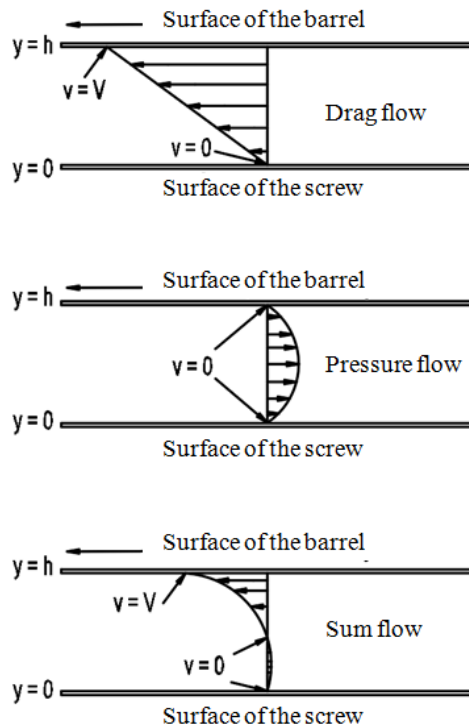


Fig. 2 - Distribution of fluid velocity in the channel of a screw

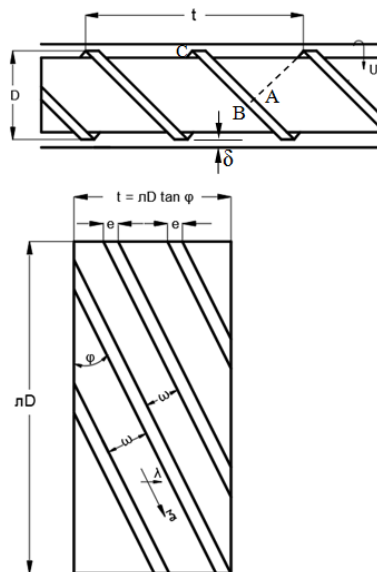


Fig. 3 - Geometry of an unrolled screw

From Fig. 3, the subsequent equations can be determined for the considered screws with any number of flights [7].

$$V = U \cos \varphi = \pi D N \cos \varphi \tag{9}$$

$$nw = (t - ne) \cos \varphi \tag{10}$$

$$w = \left(\frac{t}{n} - e\right) \cos \varphi \tag{11}$$

$$dz = \frac{d\lambda}{\sin \varphi} \tag{12}$$

Where e is the thickness of the screw, λ is the distance variable, calculated along the screw and increases in the direction of the die, t denotes the screw pitch, N denotes the screw rotation speed (rpm). Substituting Eqs. (9), (11), and (12) into Eq. (8), where n denotes the number of parallel flights of the screw, the simplified equation of the flow theory becomes:

$$Q = \frac{n\pi D N h \left(\frac{t}{n} - e\right) \cos^2 \varphi}{2} - \frac{nh^3 \left(\frac{t}{n} - e\right) \sin \varphi \cos \varphi}{12\mu} \left(\frac{dP}{dz}\right) \tag{13}$$

The most common special case of the Eq. (13) is the case of a single screw with a small screw flight width in comparison to the screw pitch t . As an illustration in Fig. 3, the pitch of the screw is calculated from the diameter as well as the helix angle using the following formula:

$$t = \pi D \tan \varphi \tag{14}$$

Eq. (15) can be derived by substituting Eq. (14) into Eq. (13). This equation is applied to the special case of the single screw ($n = 1$) where the width of the thread is omitted [14] and is obtained as:

$$Q = \frac{\pi^2 D^2 N h \sin \varphi \cos \varphi}{2} - \frac{n D h^3 \sin^2 \varphi}{12\mu} \left(\frac{dP}{dz}\right) \tag{15}$$

In Eq. (15), leak flow is ignored. The leak flow is considered to be the pressure flow that flows through a narrow gap between the screw and the barrel. The leak flow at any point on the top of the thread is constant for isothermal extrusion and uniform channel size. Hence, the total leakage flow is achieved by determining the amount of leakage per pitch. Because the same mechanism is assumed, the form of the leak-flow equation must be the same as that of the pressure-flow equation. Thus, the leak flow is proportional to the cubic power of the slit height and width, while inversely proportional to the length of the channel. The width, length, and height parameters of the slit can be inferred from Fig. 3. The height of the slit is δ . The length of the slit will be $e \cos \varphi$. The width of the slit is $\pi D / \cos \varphi$. So, the leak flow equation will be:

$$Q_L = \frac{\pi D \delta^3 E \Delta p}{12\mu e \cos^2 \varphi} \tag{16}$$

Where Δp denotes the pressure deviation from side to side of the screw thread. In Fig. 3, Δp denotes the difference in pressure between point A and point B. E denotes the eccentricity factor - assigned a value of 1. It is easier to calculate when replacing the pressure deviation on one screw top Δp with the pressure deviation over the entire screw ΔP . The pressure deviation ΔP_1 over the length of the channel equals one turn of the helix is calculated as follows [2]:

$$\Delta P_1 = \frac{\Delta P}{\text{number of turns}} = \frac{t \Delta P}{L} = \frac{\pi D \tan \varphi \Delta P}{L} \tag{17}$$

In Fig. 3, ΔP_1 denotes the difference in pressure between point A and point C. In addition, in Eq. (16), the pressure deviation from point A to point B is still required. Because of the linearity of the pressure difference in the screw channel, Δp is determined from ΔP by multiplying ΔP_1 by the ratio of the distance along the helical channel C-A to the distance B-A [7].

$$\Delta p = \frac{\pi D \tan \varphi \Delta P}{L} \left(\frac{\frac{\pi D}{\cos \varphi} - \pi D \sin \varphi \tan \varphi}{\frac{\pi D}{\cos \varphi}} \right) = \frac{\pi D \tan \varphi \cos^2 \varphi \Delta P}{L} \tag{18}$$

Where L denotes the length of the screw section which has flight. Substituting Eq. (18) into Eq. (16) and assigning E value as 1, the formula for leak flow will be written as:

$$Q_L = \frac{\pi D \delta^3 \tan \phi \Delta P}{12 \mu e L} (cm^3/s) \quad (19)$$

2.3 Screw Design

From Eq. (15), the flow of the drag flow can be determined as follows:

$$Q_D = \frac{\pi^2 D^2 N h \sin \phi \cos \phi}{2} (cm^3/s) \quad (20)$$

And the pressure flow:

$$Q_P = \frac{\pi D h^3 \sin^2 \phi}{12 \mu} \left(\frac{dP}{dz} \right) (cm^3/s) \quad (21)$$

Usually, the leak flow has a small value and is ignored [2, 7, 31]. In [32], the authors also ignored the leak flow and studied the ratio Φ between the drag flow and the pressure flow. Then, the equation for the sum flow or velocity distribution of the molten plastic flow in the screw channel had a parabolic shape according to the y position and depended on Φ . The flow velocity equals zero when $y = 0$, at the root of the considering screw. When $\Phi = 0$ ($Q_P = 0$), the velocity profile is linear because there is only the drag flow. When $\Phi > 0$, the velocity profile transforms from a line into a parabola. When $\Phi = 1/3$, the effect of the pressure flow begins to be observed. When $\Phi > 1/3$ (about $2/3$), this effect can be clearly observed [32]. Therefore, in the design of the screw, Φ is considered to be around 0.2. When $\Phi = 1$, the pressure-flow balances the opposing drag flow and the sum flow will be zero. Thus:

$$Q_P = 0.4 \pi^2 D^2 N h \sin \phi \cos \phi (cm^3/s) \quad (22)$$

Eq. (22) is the productivity of the extruder. If the design input requirement is machine capacity, from Eq. (22), the diameter of the screw required to satisfy the above requirement can be calculated.

$$D = \sqrt{\frac{Q}{0.4 \pi^2 N h \sin \phi \cos \phi}} (cm) \quad (23)$$

3. Design of Plastic Filament Extrusion Machine

3.1 Screw Diameter Calculation

Design requirements to be achieved of the machine are extrusion speed: $100 \div 200$ mm/min; plastic fiber diameter: 1.75 ± 0.1 mm. Thus, extrusion velocity:

$$v = 100 \div 200 (mm/min) = \frac{1}{6} \div \frac{1}{3} (cm/s) \quad (24)$$

Cross-section of plastic fibers, calculated according to nominal size:

$$F = \frac{\pi d^2}{4} = \frac{\pi \times 0.175^2}{4} = 0.024 (cm^2) \quad (25)$$

From Eqs. (23) and (24), the required capacity of the plastic filament extruder can be calculated as:

$$Q = v \times F = 4 \times 10^{-3} \div 8 \times 10^{-3} (cm^3/s) \quad (26)$$

For $Q = 4 \times 10^{-3} cm^3/s$, substituting this into Eq. (23) yields $D = 0.69$ cm. For $Q = 8 \times 10^{-3} cm^3/s$, substituting this into Eq. (23) yields $D = 0.87$ cm. It is worth noting that H is the flight depth in the compression and metering zones, $H = 0.2D$, and ϕ is the helix angle, $\phi = 17.60$ [33]. Thus, $D = 0.69 \div 0.87$ cm = $6.9 \div 8.7$ mm. Therefore, it is appropriate to choose to buy a screw with diameter $D = 7.9$ mm. To calculate the length of the screw, a common L/D ratio of $12/1$ [30] was chosen. Therefore, the length of the screw is:

$$L = 12 \times D = 12 \times 7.9 = 98.4(mm) \quad (27)$$

3.2 Heat Input Required for the Extrusion

Considering the overall heat exchange process in the extruder, the heat balance equation will be as follows [31] [34]:

$$Q_{ext} = Q_{cond} + Q_{conv} + Q_{rad} + Q_u \quad (28)$$

In which, Q_{ext} is the heat needed for extrusion, Q_{cond} is the heat loss due to heat conduction [35], Q_{conv} is the heat loss due to convection heat transfer, Q_{rad} is the heat loss due to heat radiation, Q_u is the amount of heat required to raise the plastic temperature from ambient to extrusion temperature. Each of the components of Eq. (28) was then analyzed. Heat loss due to heat transfer to other components, Q_{cond} , was ignored because the other components used were plastics. Heat loss due to convection heat transfer [31]:

$$Q_{conv} = h_c A(T - T_f) \quad (29)$$

h_c : Convection heat transfer coefficient. For copper, h_c is about 60-65 W.m⁻². K⁻¹ [31], h_c was chosen as 60 W.m⁻².K⁻¹; A : The heat transfer area (the surface in contact with the air), was 0.008654 m²; T : The temperature of the surface, was 333.15 K; T_f : Air temperature, was 298.15 K. Then the Eq. (29) resulted in $Q_{conv} = 70.1$ W. Loss of heat due to heat radiation [31]:

$$Q_{rad} = \sigma \varepsilon A(T^4 - T_1^4) \quad (30)$$

σ : Stefan-Boltzmann constant, which is 5.670373×10^{-8} Wm⁻²K⁻⁴; ε : The emissivity of heated copper is 0.78 [31]; T : The temperature of the surface, was 333.15 K; T_1 : Air temperature, was 298.15 K; A : The heat transfer area (the surface in contact with the air), was 0.008654 m²; Then the Eq. (29) resulted in $Q_{rad} = 1.7$ W. The heat required to raise the plastic temperature from the ambient temperature to the extrusion temperature [34]:

$$Q_u = m C_p \Delta T \quad (31)$$

m : Flow volume; ρ : Density of ABS plastic, is 1050 kg/m³ [31]; v : Extrusion speed 200 mm/min ~ 0.0033 m/s; C_p : Specific heat of plastic is 0.0016 kJ/kg °C.

$$m = \rho v F = 8.136 \times 10^{-6} (kg/s) \quad (32)$$

Substituting Eq. (32) into Eq. (31), then $Q_u = 1.8 \times 10^{-3}$ W. Thus, according to Eq. (28), the amount of heat required for extrusion was:

$$Q_{ext} = 0 + 70.1 + 1.7 + 1.8 \times 10^{-3} = 71.8(W) \quad (33)$$

Hence a heater with a capacity of 90 W was selected to ensure the heating ability.

4. Fabrication Results and Discussion

The device has been designed using NX Siemens software. The screw was tilted 45° to both utilize gravity during extrusion and ensure smooth feeding. At the same time, the feed throat was cooled by a computer fan. This cooling ensured no clumping of plastic pellets clogging the feed throat. The extruded filament was cooled by a computer fan placed in front of the extruder head. The hopper was printed by an FDM 3D printer. The device has been successfully fabricated and tested, Fig. 4. The initial test results showed that the plastic filament diameter was stable at the size of 1.74 ± 0.01 mm. Figure 5a shows the polymeric filament roll after extrusion. The wire winding was done using self-developed filament winding equipment. Figure 5b shows the measurement of ABS filament diameter using a digital caliper.

The tensile tests were then performed for two types of extruded filaments and a commercial ABS filament from Torwell®. The recycled ABS was a recycled one from industrial ABS resin; the grade was not determined. The universal tensile testing device HP-500 has a maximum load of 500 N, the precise 0.1N. A commercial ABS filament from Torwell® was used to benchmark the plastic filaments extruded from the device in this study. The resulting tensile strength of commercial ABS filament from Torwell® was approximately 40 MPa, similar to what previous studies and 3D printing websites have shown [36]. The results in Fig. 6 showed that the recycled Torwell ABS filament had a little

lower tensile force as well as elongation at break compared to the original one. While the unknown recycled ABS filament had the lowest values. It was worth noting that the variation of both the tensile force and elongation of the recycled Torwell filament was almost the same as the original one. It proved the quality of the extruded filaments. The extruded filaments were then utilized for a 3D Cubicon Single® 3D printing machine. The visualization of the printed models from the extruded filament was the same as those from the commercial filament.

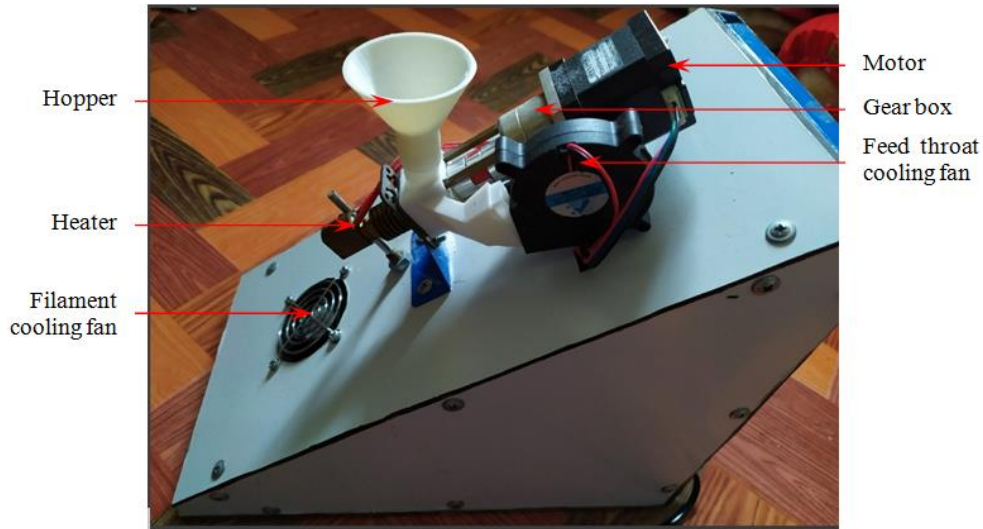


Fig. 4 - The fabricated plastic filament extruder

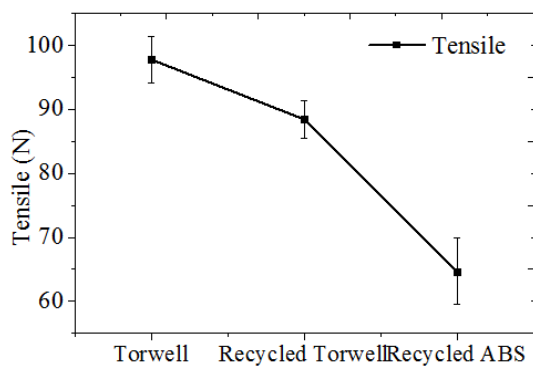


(a)

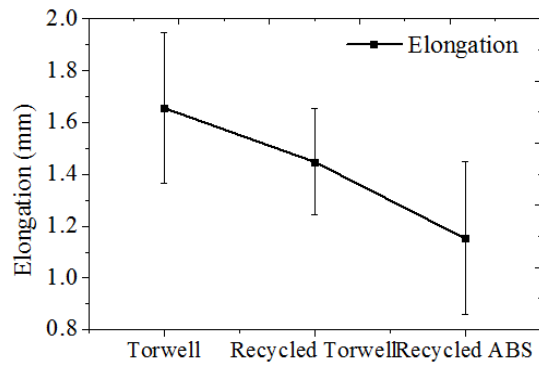


(b)

Fig. 5 - The extruded filament (a) ABS filament; (b) diameter measurement



(a)



(b)

Fig. 6 - Tensile tests for extruded filaments (a) peak tensile force; (b) maximum elongation

5. Conclusion and Suggestion

The molten plastic flow in the single screw plastic extruder has the same characteristics as the viscous liquid between two infinitely parallel sheets, one moving and one fixed. For the computational equations to be simple and applicable to both manufacturing/design and university teaching, the molten plastic was assumed to be a Newtonian fluid. A differential equation showing the relationship between the extrusion rate and the pressure at the extrusion head and the geometry of the screw and parameters of resin was established. Therefore, when the viscosity of the fluid was constant in the isothermal extrusion, the total flow of the extruder could be calculated. When the leak flow was ignored, this total flow equaled the algebraic sum of the drag flow and the pressure flow. From this extruder continuity equation, the screw diameter of the equipment can be reversed if the required extruder capacity is known. This equation for calculating screw diameter was verified via the design and fabrication of a plastic filament extruder for 3D printing. The results showed that these equations were simple enough to be applied to industrial design as well as university teaching.

To further refine this study, computational simulations using the non-Newtonian flow theory can be performed. Then a mathematical model of the extruder which is accurate enough to ignore the leak flow can be generated. With the pressure gauges for real experiments, more accurate conclusions about the formulas using Newtonian, non-Newtonian theory can be obtained and compared to experimental results.

Acknowledgement

The experiments and measurements were done by T. Q. Nguyen, N. A. T. Doan, M. H. Nguyen, N. K. Lai, T. D. Mai (DHCT13C, Faculty of Mechanical Engineering, Industrial University of Ho Chi Minh City, Ho Chi Minh City, Vietnam).

References

- [1] Li, Y., Hsieh F. (1996). Modeling of flow in a single screw extruder. *Journal of Food Engineering*, 27(4), 353-375. [https://doi.org/10.1016/0260-8774\(95\)00016-X](https://doi.org/10.1016/0260-8774(95)00016-X)
- [2] Carley J.F., Strub R.A. (1953). Basic Concepts of Extrusion. *Industrial & Engineering Chemistry*, 45(5), 970-973. <https://doi.org/10.1021/ie50521a031>
- [3] Griffith R.M. (1962). Fully Developed Flow in Screw Extruders. Theoretical and Experimental Study. *Industrial & Engineering Chemistry Fundamentals*, 1(3), 180-187. <https://doi.org/10.1021/i160003a004>
- [4] Weeks D.J., Allen W.J. (1962). Screw Extrusion of Plastics. *Journal of Mechanical Engineering Science*, 4(4), 380-400. https://doi.org/10.1243/JMES_JOUR_1962_004_051_02
- [5] Li Y., Hsieh F. (1994). New melt conveying models for a single screw extruder. *Journal of Food Process Engineering*, 17, 299-324.
- [6] Campbell G., Wang C., Hunt D., Leipold E. (1997). Screw Design and Newtonian Fluid Flow. *Journal of Reinforced Plastics and Composites*, 16, 1436-1444.
- [7] Carley J.F., Mallouk R.S., McKelvey J.M. (1953). Simplified Flow Theory for Screw Extruders. *Industrial & Engineering Chemistry*, 45(5), 974-978. <https://doi.org/10.1021/ie50521a032>
- [8] Marschik C., Dörner M., Roland W., Miethlinger J., Schöppner V., Steinbichler G. (2019). Application of Network Analysis to Flow Systems with Alternating Wave Channels: Part A (Pressure Flows). *Polymers*, 11(9). <https://doi.org/10.3390/polym11091488>
- [9] Marschik C., Roland W., Dörner M., Schaufler S., Schöppner V., Steinbichler G. (2020). Application of Network Analysis to Flow Systems with Alternating Wave Channels: Part B. (Superimposed Drag-Pressure Flows in Extrusion). *Polymers*, 12.
- [10] Rauwendaal C. (2004). Finite element studies of flow and temperature evolution in single screw extruders. *Plastics, Rubber and Composites*, 33(9-10), 390-396. <https://doi.org/10.1179/174328904X24880>
- [11] Squires P.H. (1964). Screw extrusion-flow patterns and recent theoretical developments. *Polymer Engineering & Science*, 4(1), 7-16. <https://doi.org/10.1002/pen.760040104>
- [12] Fenner R.T., Williams J.G. (1971). Some Experiments on Polymer Melt Flow in Single Screw Extruders. *Journal of Mechanical Engineering Science*, 13(2), 65-74. https://doi.org/10.1243/JMES_JOUR_1971_013_012_02
- [13] Brzoskowski R., Kubota K., Chung K., White J.L., Weissert F.C., Nakajima N., et al. (1987). Experimental and Theoretical Study of the Flow Characteristics of Rubber Compounds in an Extruder Screw. *International Polymer Processing*, 1(3), 130-136. <https://doi.org/10.3139/217.870130>
- [14] Acur E.E., Vlachopoulos J. (1982). Numerical simulation of a single screw plasticating extruder. *Polymer Engineering & Science*, 22(17), 1084-1094. doi: <https://doi.org/10.1002/pen.760221706>
- [15] Wang Y., Tsay C.C. (1996). Non - newtonian flow modeling in the mixing section of a single - screw extruder with flow analysis network method. *Polymer Engineering and Science*, 36, 643-650.

- [16] Kim N., Kim H., Lee J. (2006). Numerical analysis of internal flow and mixing performance in polymer extruder I: Single screw element. *Korea Australia Rheology Journal*, 18, 143-151.
- [17] Marschik C., Roland W., Löw-Baselli B., Miethlinger J., Kepler J., (2017). Modeling Three-Dimensional Non-Newtonian Flows in Single-Screw Extruders. Conference: ANTEC® 2017 – Anaheim, At: California, US, 1125-1130.
- [18] Wilczyński K., Buziak K., Wilczyński K.J., Lewandowski A., Nastaj A. (2018). Computer Modeling for Single-Screw Extrusion of Wood-Plastic Composites. *Polymers*, 10(3), 295. <https://doi.org/10.3390/polym10030295>
- [19] Wilczyński K., Nastaj A., Lewandowski A., Wilczyński K.J., Buziak K. (2019). Fundamentals of Global Modeling for Polymer Extrusion. *Polymers*, 11(12). <https://doi.org/10.3390/polym11122106>
- [20] Hyvärinen M., Jabeen R., Kärki T. (2020). The Modelling of Extrusion Processes for Polymers-A Review. *Polymers*, 12(6), 1306. <https://doi.org/10.3390/polym12061306>
- [21] Gibson I., Rosen D., Stucker B. (2015). Introduction and Basic Principles. In: Gibson I, Rosen D, Stucker B, editors. *Additive Manufacturing Technologies: 3D Printing, Rapid Prototyping, and Direct Digital Manufacturing*. New York, NY: Springer New York, pp. 1-18.
- [22] Maidin S., Ting K.H., Sim Y.Y. (2022). Investigation of Mechanical Properties of Recycled ABS Printed with Open Source FDM Printer Integrated with Ultrasound Vibration. *International Journal of Integrated Engineering*, 14(4), 57-63. <https://doi.org/10.30880/ijie.2022.14.04.006>
- [23] Huynh T.T., Nguyen T.V.T., Nguyen Q.M., Nguyen T.K. (2021). Minimizing Warpage for Macro-Size Fused Deposition Modeling Parts. *Computers, Materials & Continua*, 68(3). <https://doi.org/10.32604/cmc.2021.016064>
- [24] Sukindar N.A., Mohd Samsudin N., Syed Shaharuddin S.I., Kamaruddin S. (2022). The Effects of FDM Printing Parameters on the Compression Properties of Polymethylmethacrylate (PMMA) using Finite Element Analysis. *International Journal of Integrated Engineering*, 14(2), 86-92. <https://doi.org/10.30880/ijie.2022.14.02.013>
- [25] Boparai K.S., Singh R. (2019). Development of Rapid Tooling Using Fused Deposition Modeling. In: AlMangour B, editor. *Additive Manufacturing of Emerging Materials*. Cham: Springer International Publishing, pp. 251-277.
- [26] Harimalairajan K., Sadhananthan S., Murugan S. (2016). Development of Plastic Filament Extruder for 3D Printing. *International Journal of Mechanical And Production Engineering*, 4(11), 32-35.
- [27] Woern A.L., McCaslin J.R., Pringle A.M., Pearce J.M. (2018). RepRapable Recyclebot: Open source 3-D printable extruder for converting plastic to 3-D printing filament. *HardwareX*, 18, 4:e00026. <https://doi.org/10.1016/j.ohx.2018.e00026>
- [28] Mohammed M.I., Wilson D., Gomez-Kervin E., Vidler C., Rosson L., Long J. (2018). The recycling of E-Waste ABS plastics by melt extrusion and 3 D printing using solar powered devices as a transformative tool for humanitarian aid. 2018 International Solid Freeform Fabrication Symposium, 80-92. <http://dx.doi.org/10.26153/tsw/17001>
- [29] Whyman S., Arif K.M., Potgieter J. (2018). Design and development of an extrusion system for 3D printing biopolymer pellets. *The International Journal of Advanced Manufacturing Technology*, 96(9), 3417-3428. <https://doi.org/10.1007/s00170-018-1843-y>
- [30] Giles H.F., Wagner J.R., Mount E.M. (2005). 5 - Screw Design. In: Giles HF, Wagner JR, Mount EM, editors. *Extrusion*. Norwich, NY: William Andrew Publishing, pp. 53-63.
- [31] Lienhard J. (2013). *A Heat Transfer Textbook*: Phlogiston Press, Cambridge.
- [32] Vlachopoulos J., Strutt D. (2012). The Role of Rheology in Polymer Extrusion. *Materials Science*, 1-25.
- [33] Dealy J.M., Wissbrun K.F. (1999). Role of Rheology in Extrusion. In: Dealy JM, Wissbrun KF, editors. *Melt Rheology and Its Role in Plastics Processing: Theory and Applications*. Dordrecht: Springer Netherlands, pp. 441-490.
- [34] Nguyen T.K., Lee B.-K. (2018). Post-processing of FDM parts to improve surface and thermal properties. *Rapid Prototyping Journal*, 24(7), 1091-1100. <https://doi.org/10.1108/RPJ-12-2016-0207>
- [35] Verros G.D. (2020). Comprehensive Criteria for the Extrema in Entropy Production Rate for Heat Transfer in the Linear Region of Extended Thermodynamics Framework. *Axioms*, 9(4). <https://doi.org/10.3390/axioms9040113>
- [36] Samykano, M., Selvamani, S.K., Kadirgama, K. et al. (2019). Mechanical property of FDM printed ABS: influence of printing parameters. *Int J Adv Manuf Technol* 102, 2779–2796. <https://doi.org/10.1007/s00170-019-03313-0>